Cross Section Measurements of Polarized $W^{\pm}W^{\pm}$ Scattering in Fully Leptonic Decay with the CMS Detector

Miao Hu

on behalf of the CMS collaboration

2020-Oct-9th
LHC EW WG General Meeting

Motivation: Theoretical

- Discovery of the **Higgs Boson**
  - Consistent with the standard model (SM)
  - Heavy vector bosons W and Z acquire their mass through the Brout–Englert–Higgs mechanism

- **Polarization** of the massive vector boson
  - Three modes: one longitudinally and two transverse

$$\epsilon^{\mu}_{T_1,T_2} = \frac{1}{\sqrt{2}}(0,1,\pm i,0) \qquad \epsilon^{\mu}_{L} = \frac{1}{m}(k_3,0,0,E)$$

  - **Longitudinal polarization** is a consequence of the **Electroweak Symmetry Breaking Mechanism (EWSB)**
  - The **unitarity** of the **longitudinally polarized** vector boson scattering (VBS) at high energies is **restored** in the SM by **a Higgs boson with a mass < 1 TeV**

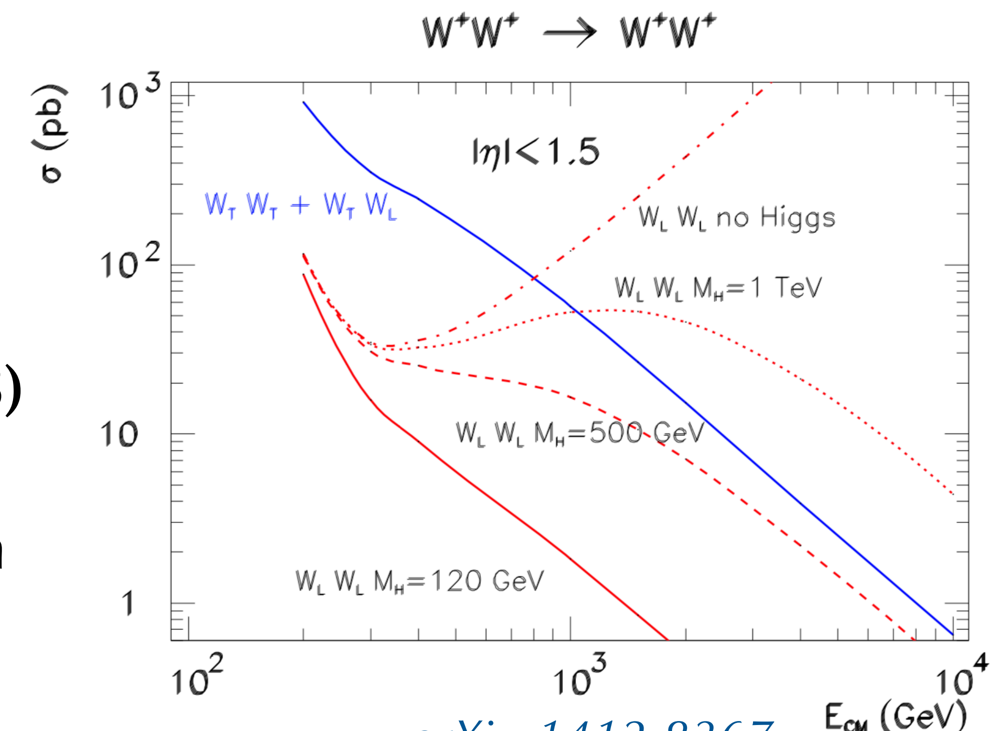

arXiv:1412.8367

- The discovered Higgs boson the lone player responsible for EWSB?

- The polarized VBS amplitudes at high energies is sensitive not only to the **Higgs mass**, but also to **Higgs-to-Vector-Boson couplings**, and the **triple and quartic vector boson couplings**

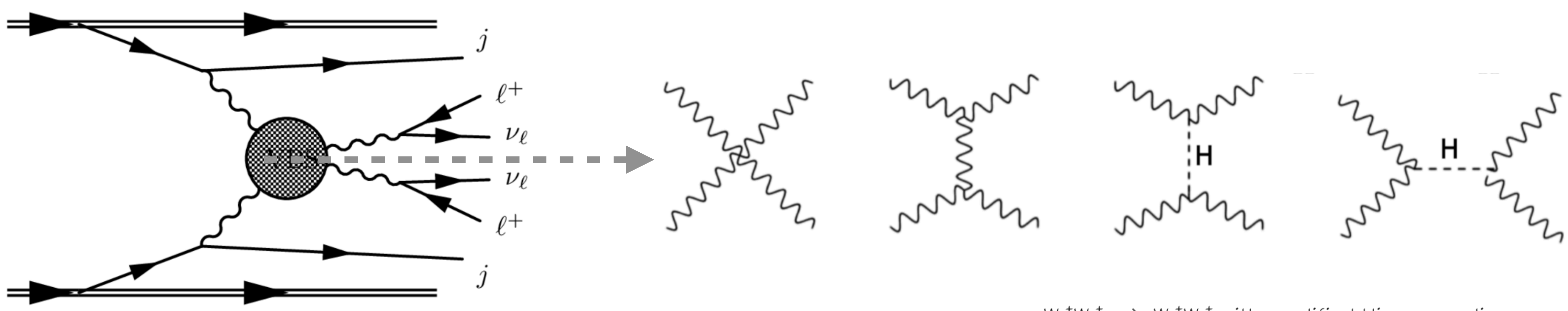

- Provide complementary information to direct Higgs boson measurements
  - Excess in the longitudinally polarized VBS cross section would point to new physics in the EWSB sector

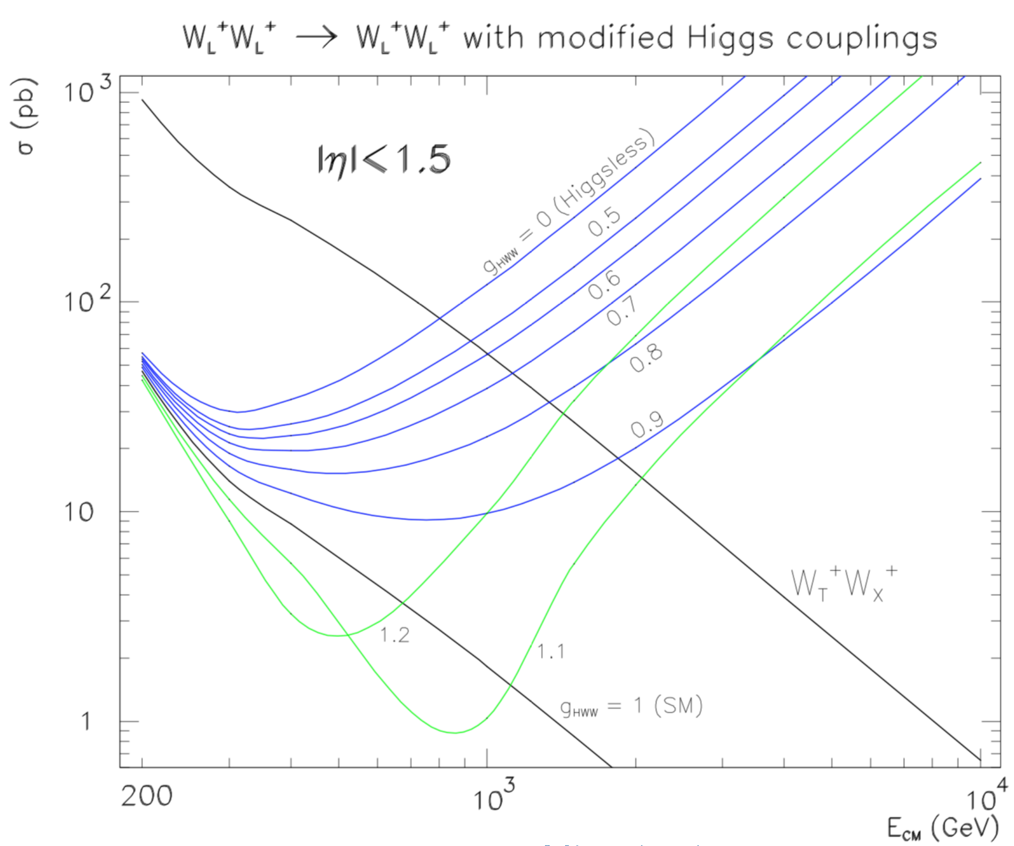

arXiv:1412.8367

Motivation: Experimental

- **First measurement** of the EW production cross sections of the **polarized VBS**!
  - The longitudinal scattering contributes to about ~10% of the overall EW production
  - LHC Full Run 2 luminosities of 137.1 fb^{-1} at 13 TeV open up possibilities for precise measurements of electroweak boson production processes
  - One of the high profile analyses for HL-LHC

phys.lett.b.2020.135710

- CMS-SMP-19-012: the most precise measurement of EW $W^{\pm}W^{\pm}$ cross section to date
  - Follow the same studies

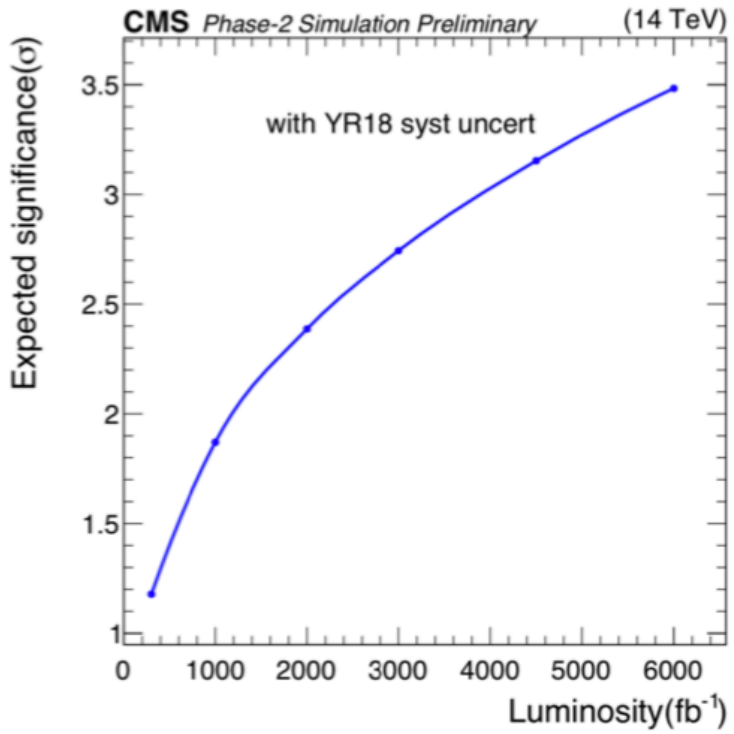

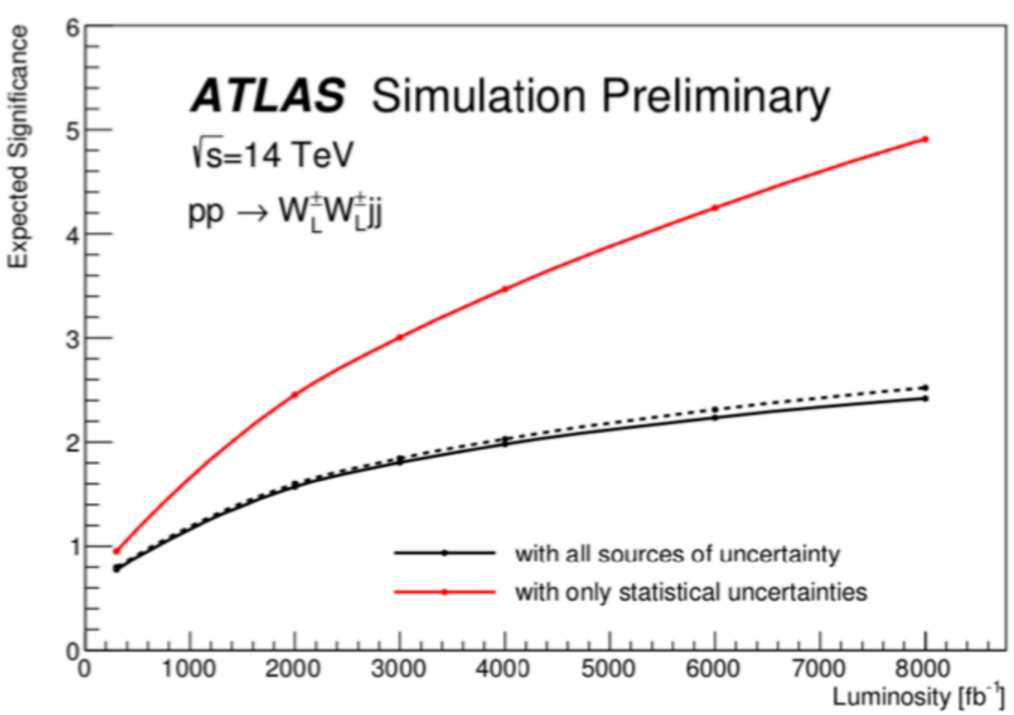

VBS in Leptonic Channel Overview

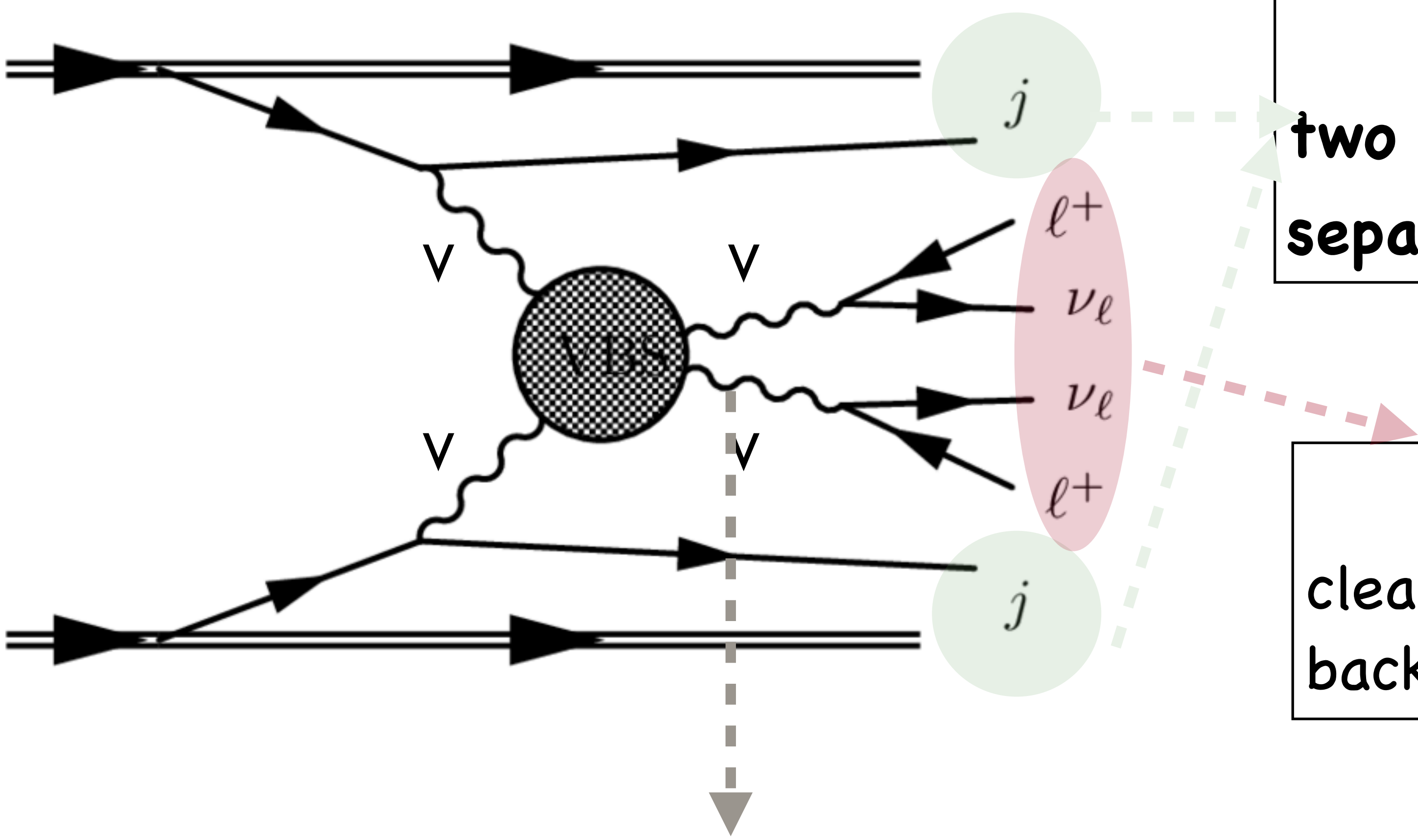

VBS Signature

two forward **jets** with large **rapidity separation** and **dijet mass**

Fully Leptonic decay

cleaner final states hence lower backgrounds

Uniqueness of Same Sign

- EW production dominant over QCD-induced
- In particular for **polarization VBS**
  - the only process for which the cross-talk amplitudes: $W_X W_T \rightarrow W_L W_L$ and $W_L W_L \rightarrow W_X W_T$ are completely negligible

W±W± & WZ scattering: Strategy

CMS-SMP-19-012 *phys.lett.b.2020.135710*

- **Event selection** based on the signature of **VBS** and two($W^{\pm}W^{\pm}$)/three(WZ) isolated **leptons**
- **Background estimation**: A combination of
  - **data-driven** methods with background-enriched control regions (CRs) selected by inverting some of event selection requirements
  - **simulated** studies
- A **multivariate analysis** is used to better separate the **EW WZ** from QCD WZ processes
- The **EW $W^{\pm}W^{\pm}$** and **WZ** production cross sections are measured by **simultaneously fitting** of several distributions (m_{jj}, $m_{\ell\ell}$, BDT Score…) across all SRs and CRs

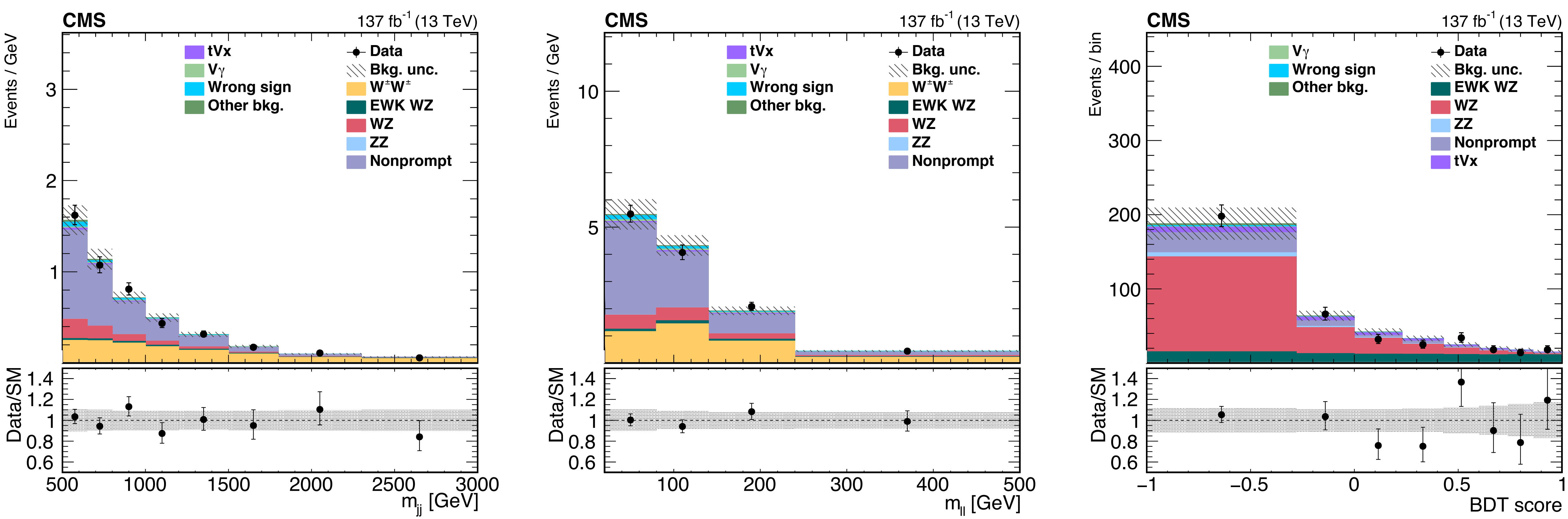

$W^{\pm}W^{\pm}$ & WZ scattering: Results

CMS-SMP-19-012 *phys.lett.b.2020.135710*

- Observed(Expected) **significance**
  - EWK WZ : 6.8 (5.3)σ
  - EWK WW : far above 5σ

- **Inclusive cross section** measurements

Process	$\sigma\mathcal{B}$ (fb)	Theoretical prediction without NLO corrections (fb)	Theoretical prediction with NLO corrections (fb)
EW $W^{\pm}W^{\pm}$	3.98 ± 0.45 $0.37\,(\text{stat}) \pm 0.25\,(\text{syst})$	3.93 ± 0.57	3.31 ± 0.47
EW+QCD $W^{\pm}W^{\pm}$	4.42 ± 0.47 $0.39\,(\text{stat}) \pm 0.25\,(\text{syst})$	4.34 ± 0.69	3.72 ± 0.59
EW WZ	1.81 ± 0.41 $0.39\,(\text{stat}) \pm 0.14\,(\text{syst})$	1.41 ± 0.21	1.24 ± 0.18
EW+QCD WZ	4.97 ± 0.46 $0.40\,(\text{stat}) \pm 0.23\,(\text{syst})$	4.54 ± 0.90	4.36 ± 0.88
QCD WZ	3.15 ± 0.49 $0.45\,(\text{stat}) \pm 0.18\,(\text{syst})$	3.12 ± 0.70	3.12 ± 0.70

- Absolute and normalized **differential cross section** measurements on m_{jj}, $m_{\ell\ell}$, p_T^{max} for $W^{\pm}W^{\pm}$ and m_{jj} for WZ

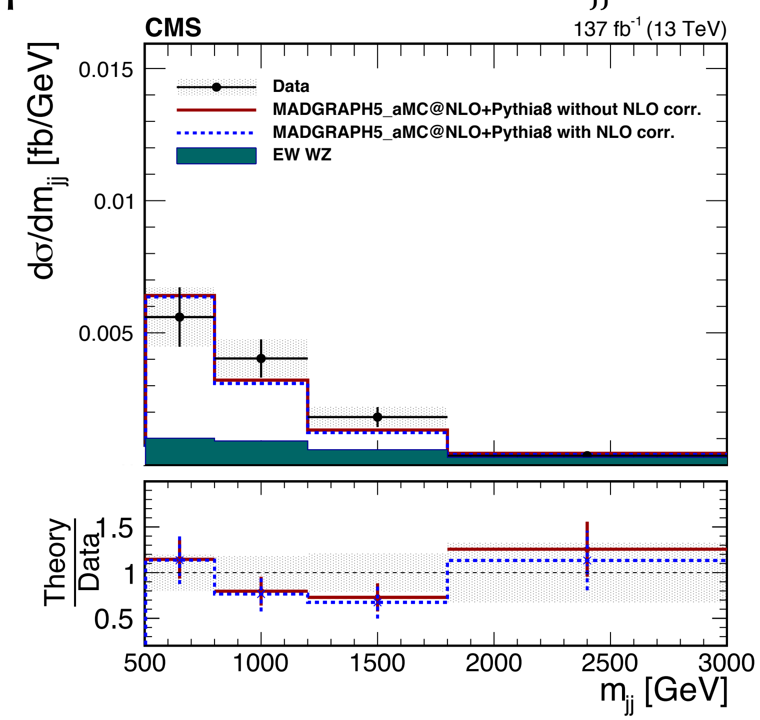

WZ

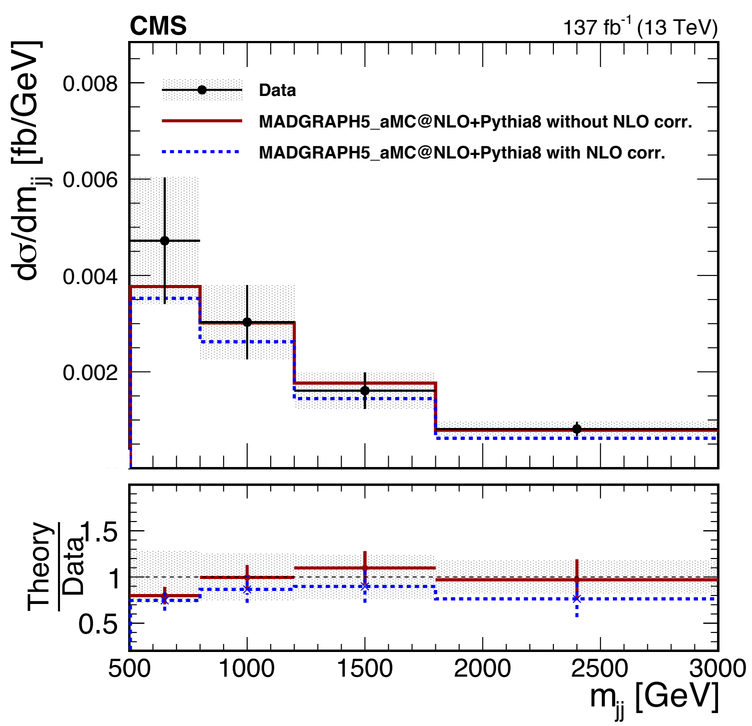

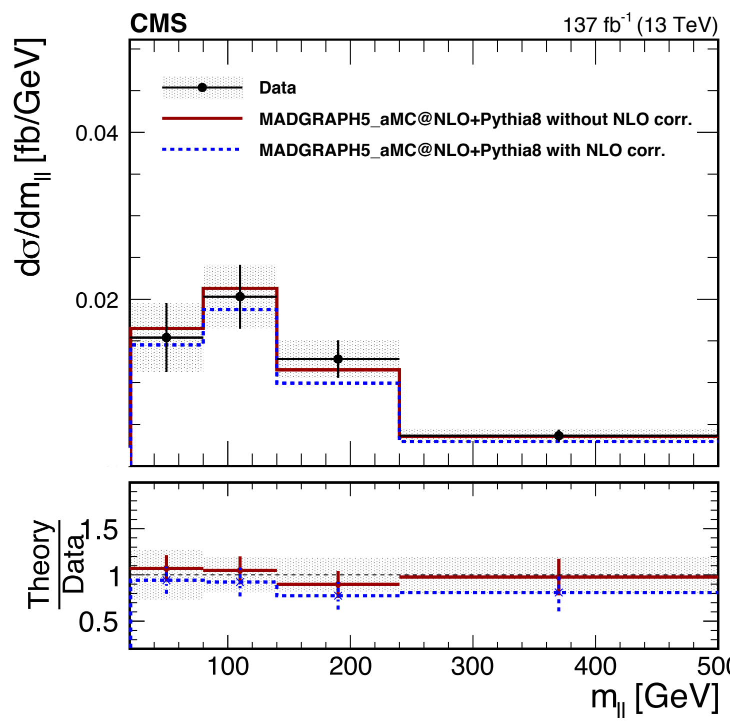

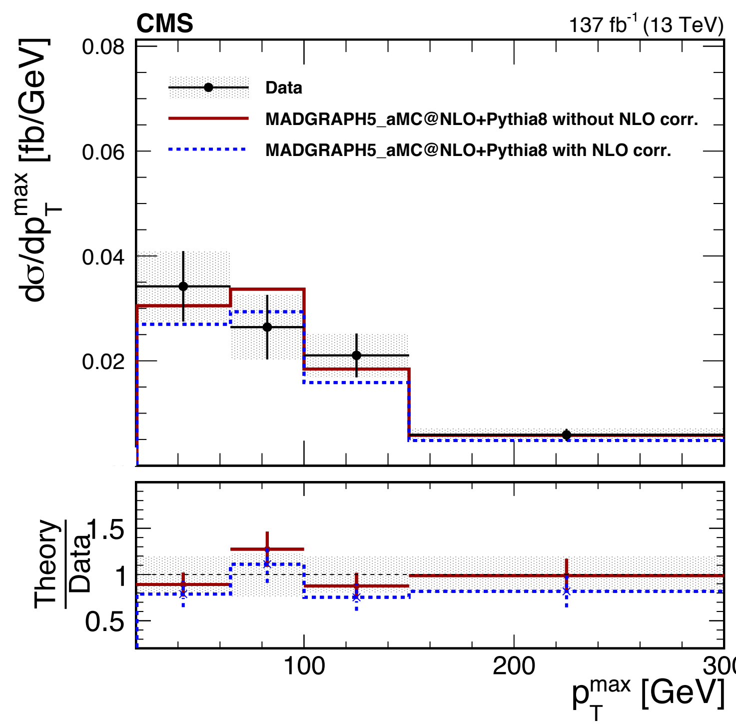

$W^{\pm}W^{\pm}$

Polarized $W^{\pm}W^{\pm}$ scattering: Overview

- Polarization configurations: EW $W_L^{\pm}W_L^{\pm}$ (**LL**), $W_L^{\pm}W_T^{\pm}$(**LT**) and $W_T^{\pm}W_T$(**TT**)

- Measurements
  - **Ideally, measure all three contributions separately**
    - Unreliable currently due to limited data sample size
  - **Provide two maximum-likelihood fits**
    - **(i) LL and XT (X = L or T)**
    - **(ii) LX and TT (X = L or T)**
  - Two sets of results are reported with the helicity eigenstates defined
    - (i) in the **$W^{\pm}W^{\pm}$ center-of-mass (c.m.) frame**
    - (ii) in the initial-state **parton-parton c.m frame**

Signal Samples

- Signals are simulated at LO using MADGRAPH5_aMC@NLO 2.7.2 with automated predictions of polarized scattering arXiv 1912.01725
  - Two sets of samples are generated
    - With the helicity eigenstates defined either in the $\mathbf{W^{\pm}W^{\pm}}$ c.m. reference frame or in the initial **parton-parton** reference frame
  - Good agreement with polarized samples produced using PHANTOM 1.5.1generator

- Generated samples with $m_{jj} > 200$ GeV and $p_T^j > 10$ GeV
  - For each year separately
  - For each polarization configuration separately

Mode	σ parton-parton frame (fb/%)	σ WW frame (fb/%)
$W_L W_L$	2.119 / 7.3	3.193 / 10.9
$W_L W_T$	10.87 / 37.4	9.288 / 31.9
$W_T W_T$	16.10 / 55.3	16.67 / 57.2
Total	29.1 / 100	29.1 / 100

Closure of signal samples

- Follow the same selections as that for the fiducial regions (Slide p20)
- Good agreement between incoherent sum of the polarized cross sections and for the unpolarized cross sections for the distributions of the observables ($\Delta\Phi_{jj}$, $\Delta\Phi_{ll}$, m_{ll})

WW frame | parton-parton frame

$\Delta\Phi_{jj}$

$\Delta\Phi_{ll}$

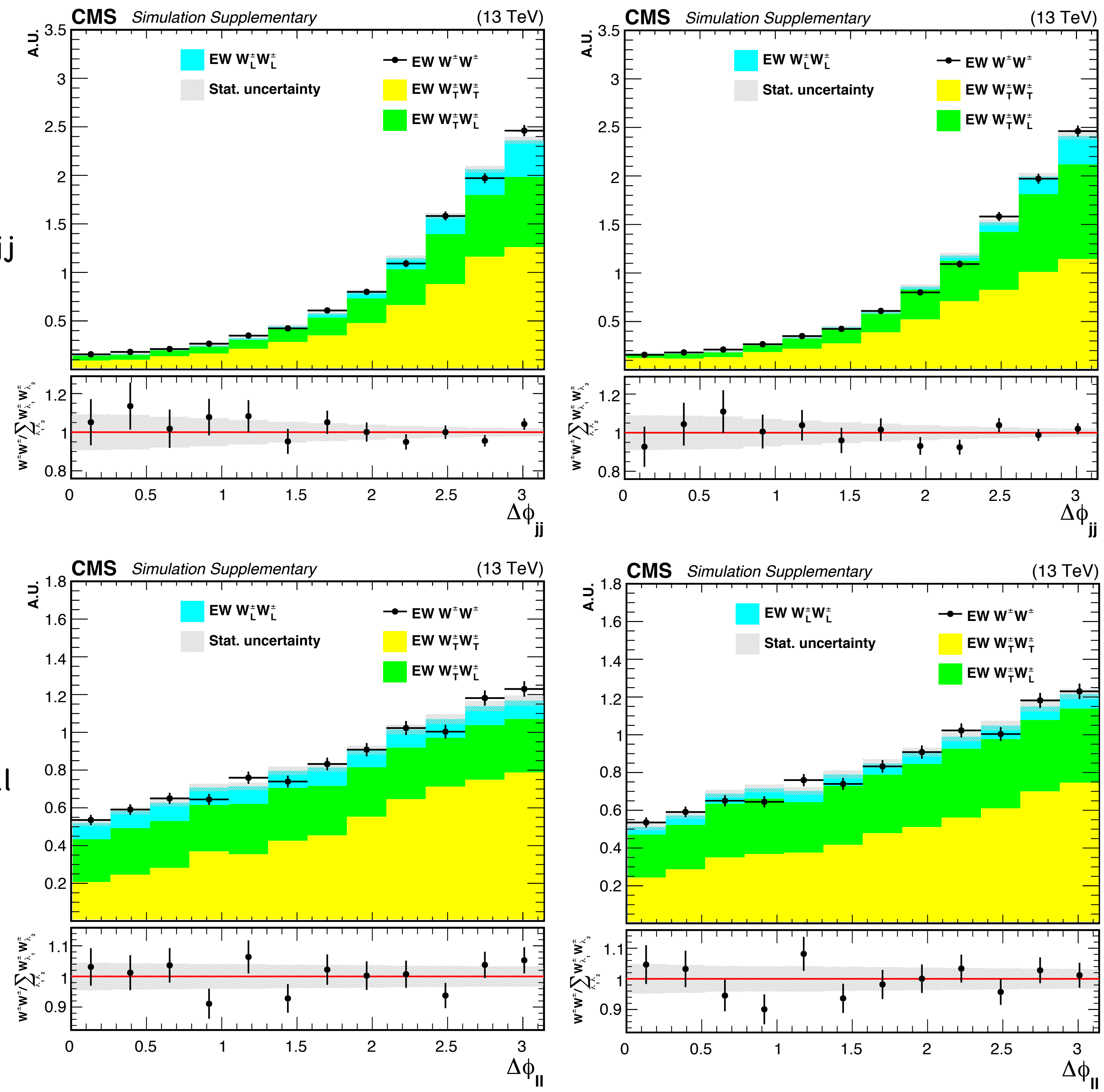

NLO corrections

- The full NLO QCD and EW corrections for the leptonic unpolarized $W^{\pm}W^{\pm}$ scattering have been computed *B.Biedermann, A.Denner, and M.Pellen* *arXiv:1611.02951* *arXiv:1708.00268*
- Reduce the LO cross section for the EW $W^{\pm}W^{\pm}$ process by approximately 10–15%
- Unknown for LL, LT, TT processes
  - α_s corrections expected to be the **same for all the 3** polarization modes
  - α corrections expected to be **small for the L** mode
  - Take the NLO corrections for the unpolarized EW $W^{\pm}W^{\pm}$ and apply
    - $\mathcal{O}(\alpha_s\alpha^6)$ and $\mathcal{O}(\alpha^7)$ to **TT**
    - Only $\mathcal{O}(\alpha_s\alpha^6)$ to **LL** and **LT**
    - $\mathcal{O}(\alpha^7)$ on the shapes of **LL** and **LT** considered as a systematic uncertainty

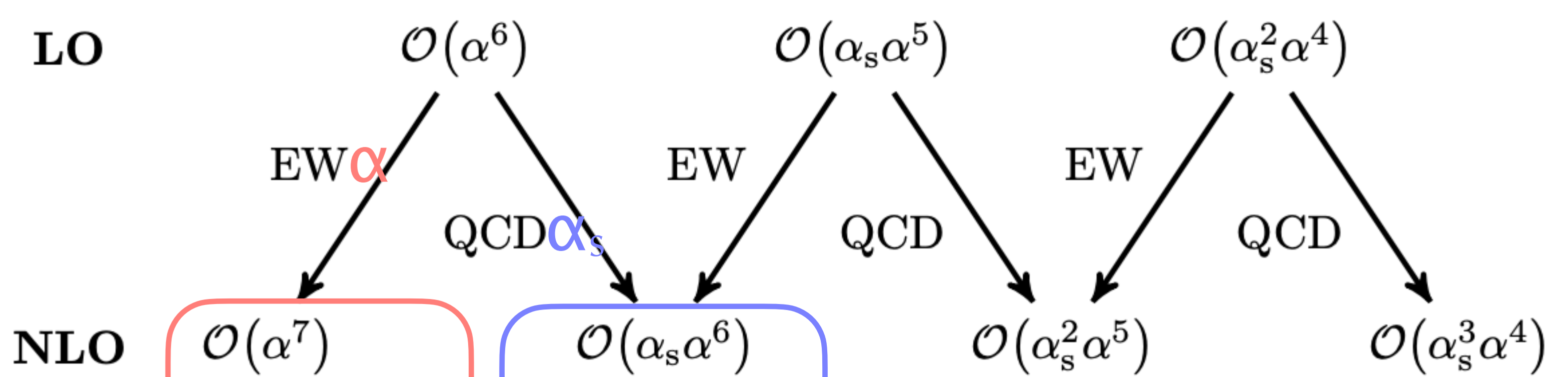

Order	$\mathcal{O}(\alpha^7)$	$\mathcal{O}(\alpha_s\alpha^6)$	$\mathcal{O}(\alpha_s^2\alpha^5)$	$\mathcal{O}(\alpha_s^3\alpha^4)$	Sum
$\delta\sigma_{\mathrm{NLO}}$ [fb]	−0.2169(3)	−0.0568(5)	−0.00032(13)	−0.0063(4)	−0.2804(7)
$\delta\sigma_{\mathrm{NLO}}/\sigma_{\mathrm{LO}}$ [%]	−13.2	−3.5	0.0	−0.4	−17.1

Event Selection

Follow the same selections in CMS-SMP-19-012 *phys.lett.b.2020.135710*

Variable	Selections
leptons	2 SS, P_T > 25/20 GeV
$\|m_{\ell\ell} - m_Z\|$	> 15 GeV for ee
$m_{\ell\ell}$	> 20 GeV
$m_{\ell\ell\ell}$	-
p_T^j	> 50GeV
p_T^{miss}	> 30 GeV
Anti b-tagging	applied
tau veto	applied
max(z^*_ℓ) $z^*_\ell = \|\eta_\ell - (\eta_{j1} + \eta_{j2})/2\| / \|\Delta\eta_{jj}\|$	<0.75
m_{jj}	> 500GeV
$\|\Delta\eta_{jj}\|$	> 2.5

lepton selections and requirements

VBS signature

MVA Analysis

- Multivariate techniques are used to enhance the separation between different processes

- Two sets of BDTs are trained
  - **Signal BDTs** to separate different polarization configurations
    - Two settings
      - (i) **LL** against **(LT+TT)**
      - (ii) **(LL+LT)** against **TT**
    - Different polarization states lead to different kinematic distributions
      - Example: smaller p_T of W_T compared to p_T of the radiated W_T
    - Different trainings for parton-parton and WW c.m. frame

  - **Inclusive BDT** to isolate EW $W^{\pm}W^{\pm}$ signal from nonVBS backgrounds
    - NonVBS backgrounds are dominated by non-prompt ttbar events

- Three categories of discriminating variables
  - Jet kinematics, vector boson kinematics, and Vector boson - jet mix variables
  - 15 for Signal BDT (BackUp P32), 10 for inclusive BDT (BackUp P33)

Signal BDTs

- Distributions of three variables with great separation power are shown
- Different between LL and XT, between LX and TT (X=L or T)

$\Delta\Phi_{jj}$ | $\Delta\Phi_{ll}$ | m_{ll}

parton-parton frame

WW frame

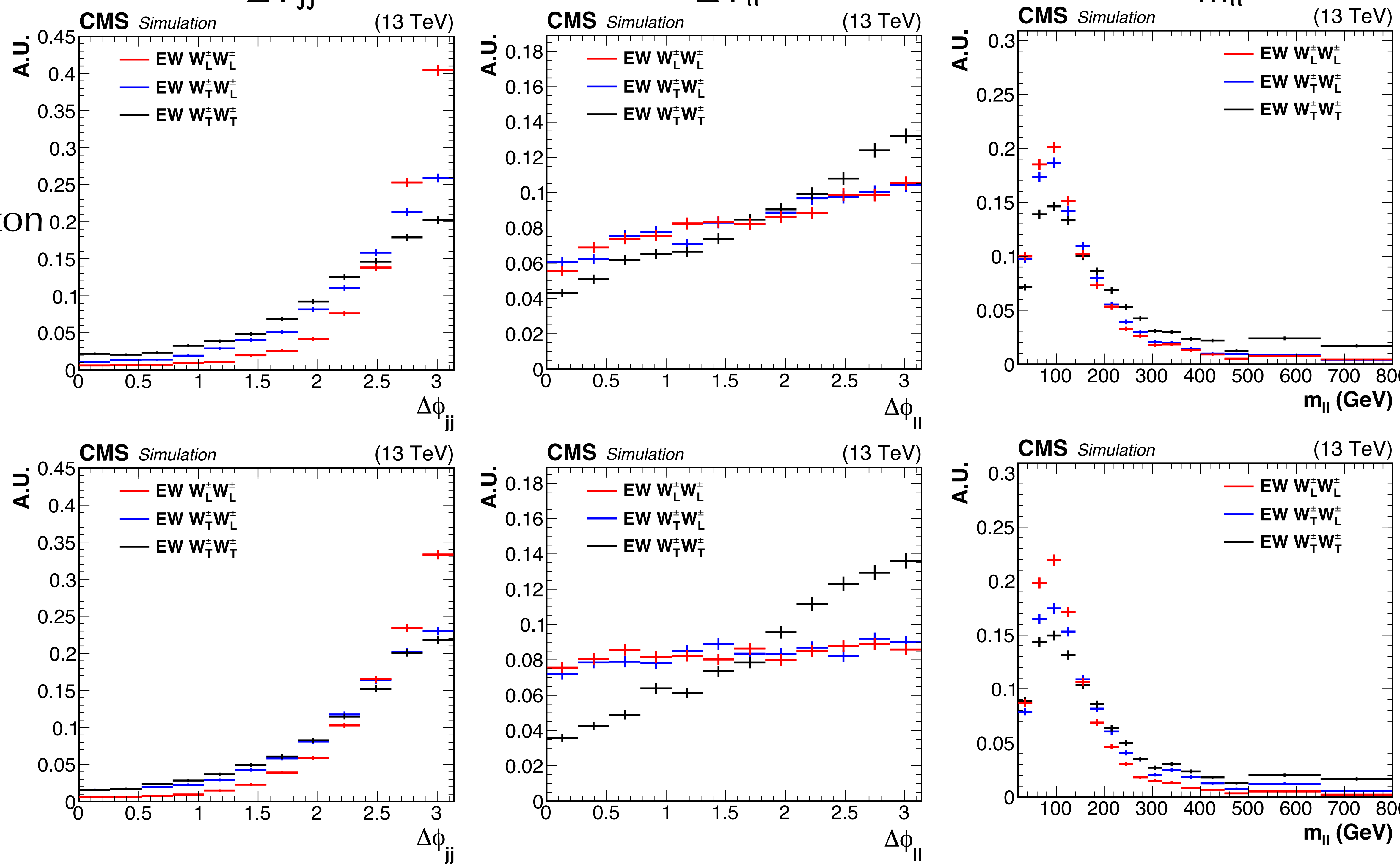

Background estimation

- A combination of **data-driven** methods and detailed **simulated** studies to estimate backgrounds

Follow the same as in CMS-SMP-19-012 *phys.lett.b.2020.135710*

Category	Estimation	Contribution
WW QCD	From simulation	
WW DPS	From simulation	
WZ	✦ From simulation	~ 15%
Tribosons	From simulation	
WZb(tZq)	✦ From simulation	
ZZ	✦ From simulation	
Nonprompt	From fake rates and "Tight+Loose" "Loose+Loose" data events	~ 60%
Wrong-sign	From charge mis-ID S.F.s and simulated OS events	

- Backgrounds estimated from simulation marked with ✦ have normalization assessed from data, others are normalized to the best theoretical cross section prediction
- In all cases where simulation is used, events are reweighted to correct for the pileup, lepton and trigger efficiencies to agree with the data distribution

Signal Extraction

- Several control regions (CRs) are defined by inverting certain selections
- Simultaneously fit on several distributions across all signal and control regions
  - SR: 2D of signal BDT X inclusive BDT
  - CR: m_{jj}

Follow the same as in CMS-SMP-19-012 *phys.lett.b.2020.135710*

Variable	SSWW SR	Nonprompt CR	WZ CR	WZb CR	ZZ CR
leptons	2 SS, $P_T > 25/20$ GeV	2 SS, $P_T > 25/20$ GeV	1 OS pair + 1, $P_T >$ 25/10/20 GeV	1 OS pair + 1, $P_T >$ 25/10/20 GeV	2 OS pairs, $P_T >$ 25/20/10/10GeV
$\lvert m_{\ell\ell} - m_Z \rvert$	> 15 GeV (ee)	> 15 GeV (ee)	< 15 GeV	< 15 GeV	< 15 GeV(both pairs)
$m_{\ell\ell}$	> 20 GeV	> 20 GeV	-	-	-
$m_{\ell\ell\ell}$	-	-	>100GeV	>100GeV	-
p_T^j	> 50GeV	> 50GeV	> 50GeV	> 50GeV	-
p_T^{miss}	> 30 GeV	> 30 GeV	> 30 GeV	> 30 GeV	-
Anti b-tagging	applied	Inverted	applied	Inverted	-
tau veto	applied	applied	applied	applied	-
$\max(z^*_\ell)$	<0.75	<0.75	<1.0	<1.0	<0.75
m_{jj}	> 500GeV	> 500GeV	> 500GeV	> 500GeV	> 500GeV
$\lvert \Delta\eta_{jj} \rvert$	> 2.5	> 2.5	> 2.5	>2.5	> 2.5

- The predicted yields are shown with their best fit normalizations from the simultaneous fit
- The histograms for the $W^{\pm}W^{\pm}$ process include the contributions from the EW $W_L^{\pm}W_L^{\pm}$, $W_L^{\pm}W_T^{\pm}$ and $W_T^{\pm}W_T^{\pm}$ processes (shown as solid lines), QCD $W^{\pm}W^{\pm}$ and interference
- in WW c.m. frame

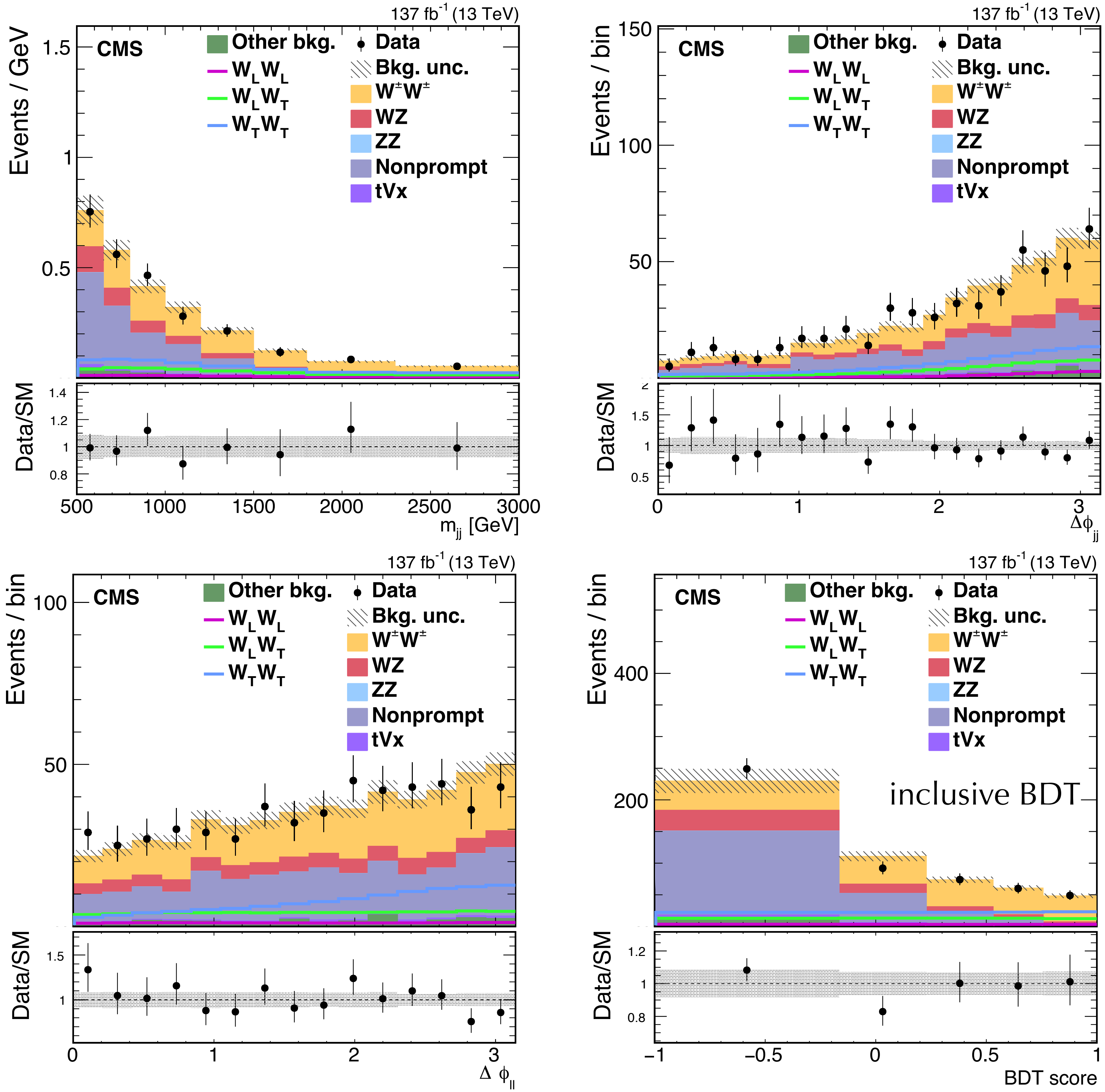

- Two signal BDT scores ((i)LL and (LT+TT) (ii) (LL+LT) and TT) are shown
- The predicted yields in SR are shown with their best fit normalizations from the simultaneous fit for (i) LL and (LT+TT) cross sections
  - The LT and TT yields are obtained from the XT yields assuming the SM prediction for the ratio of the two
  - in WW c.m. frame

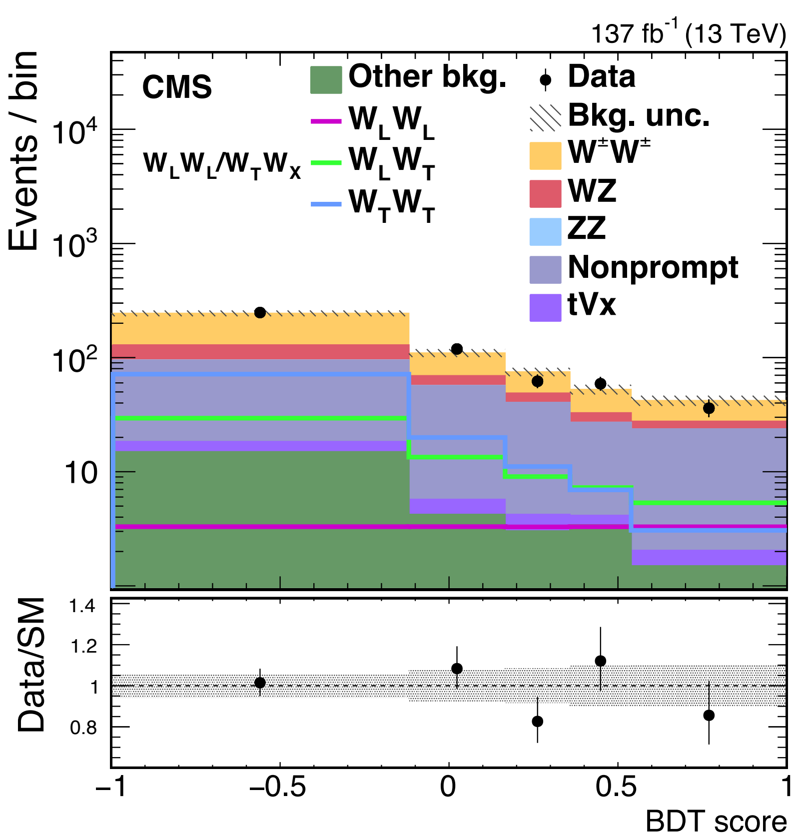

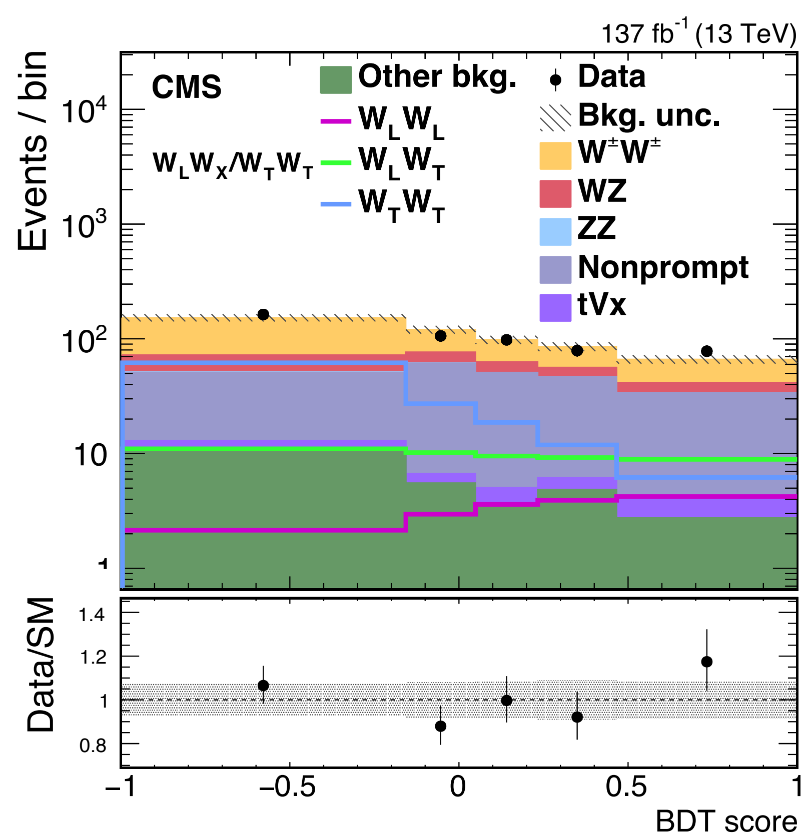

Process	Yields in $W^\pm W^\pm$ SR
$W^\pm_L W^\pm_L$	16.0 ± 18.3
$W^\pm_L W^\pm_T$	63.1 ± 10.7
$W^\pm_T W^\pm_T$	110.1 ± 18.1
QCD $W^\pm W^\pm$	13.8 ± 1.6
Interference $W^\pm W^\pm$	8.4 ± 0.6
WZ	63.3 ± 7.8
ZZ	0.7 ± 0.2
Nonprompt	213.7 ± 52.3
tVx	7.1 ± 2.2
Other background	26.9 ± 9.9
Total SM	522.9 ± 60.7
Data	524

in WW c.m. frame

Systematics Uncertainties

- Systematic uncertainties of polarized $W^{\pm}W^{\pm}$ scattering cross section measurements are shown
  - In both LL v.s. XT , and LX v.s.TT
- Measurements are statistically dominated

Source of uncertainty	$W_L^{\pm}W_L^{\pm}$ (%)	$W_X^{\pm}W_T^{\pm}$ (%)	$W_L^{\pm}W_X^{\pm}$ (%)	$W_T^{\pm}W_T^{\pm}$ (%)
Integrated luminosity ✱ ✦	3.2	1.8	1.9	1.8
Lepton measurement	3.6	1.9	2.5	1.8
Jet energy scale and resolution ✱	11	2.9	2.5	1.1
Pileup	0.9	0.1	1.0	0.3
b tagging	1.1	1.2	1.4	1.1
Nonprompt lepton rate	17	2.7	9.3	1.6
Trigger ✱	1.9	1.1	1.6	0.9
Limited sample size ✱	38	3.9	14	5.7
Theory	6.8	2.3	4.0	2.3
Total systematic uncertainty	44	6.6	18	7.0
Statistical uncertainty	123	15	42	22
Total uncertainty	130	16	46	23

statistically limited !

✱ Uncorrelated among years
✦ affect only normalizations

Results

- Negative profile log-likelihood as a function of LL cross section
  - 95% CL upper limits obtained from the profile likelihood ratio scan

- WW c.m. frame
  - Observed (expected) significance of **2.3 (3.1)** $\boldsymbol{\sigma}$ for $\mathbf{W_L^{\pm}W_X^{\pm}}$ production
  - Observed (expected) limit of **1.17 (0.88) fb** for $\mathbf{W_L^{\pm}W_L^{\pm}}$ production
- Parton-parton c.m. frame
  - Observed (expected) significance of **2.6 (2.9)** $\boldsymbol{\sigma}$ for $\mathbf{W_L^{\pm}W_X^{\pm}}$ production
  - Observed (expected) limit of **1.06 (0.85) fb** for $\mathbf{W_L^{\pm}W_L^{\pm}}$ production

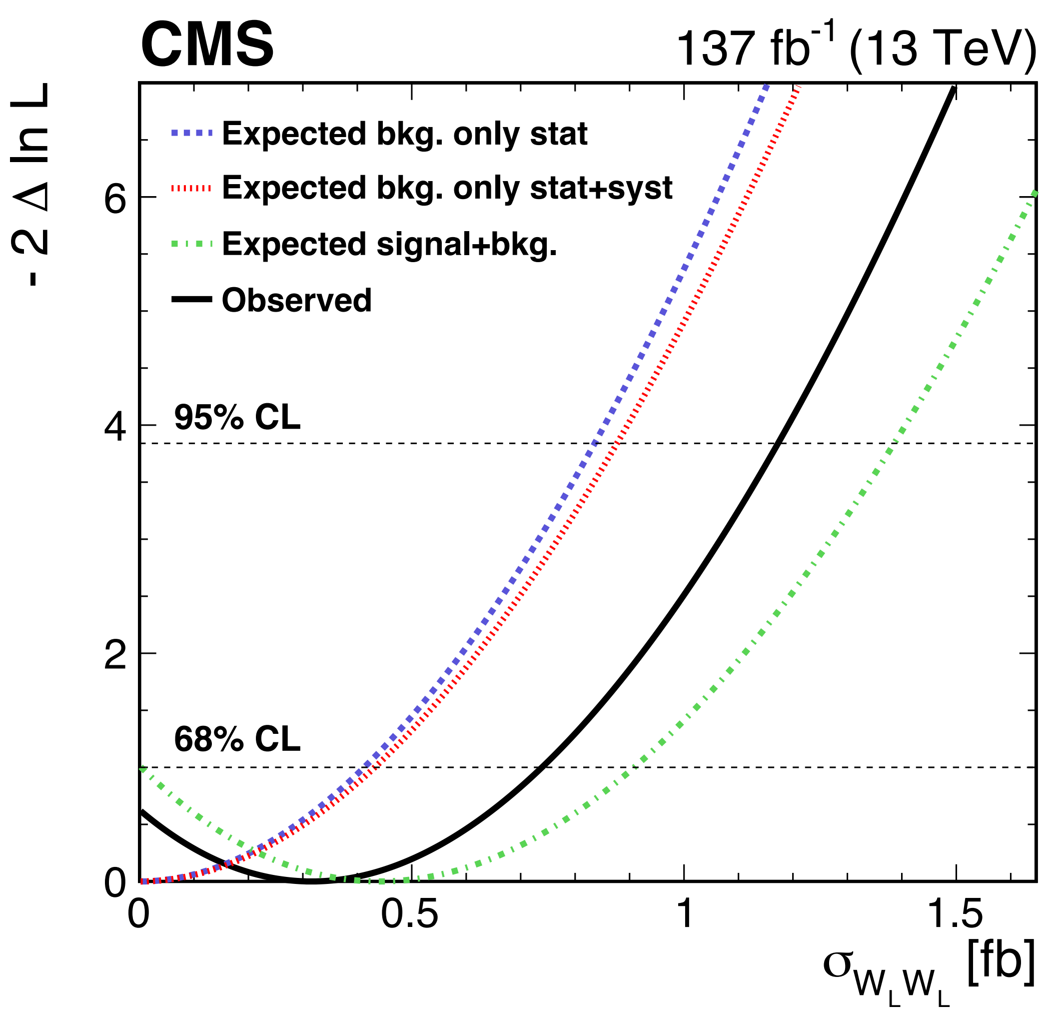

Results: Cross section measurements

- Propose fiducial regions defined as
  - Two SS leptons: $p_T > 20$ GeV, $|\eta| < 2.5$, $m_{ll} > 20$ GeV
  - Two jets: $p_T > 50$ GeV, $|\eta| < 4.7$, $m_{jj} > 500$ GeV, $|\Delta\eta_{jj}| > 2.5$

- Fiducial cross sections measured for
  - (i)LL and (LT+TT) (ii) (LL+LT) and TT
  - In both WW c.m and parton-parton c.m frame
  - Good agreement with the theoretical predictions within uncertainties

WW frame

Process	$\sigma\mathcal{B}$ (fb)	Theoretical prediction (fb)
$W^\pm_L W^\pm_L$	$0.32^{+0.42}_{-0.40}$	0.44 ± 0.05
$W^\pm_X W^\pm_T$	$3.06^{+0.51}_{-0.48}$	3.13 ± 0.35
$W^\pm_L W^\pm_X$	$1.20^{+0.56}_{-0.53}$	1.63 ± 0.18
$W^\pm_T W^\pm_T$	$2.11^{+0.49}_{-0.47}$	1.94 ± 0.21

parton-parton frame

Process	$\sigma\mathcal{B}$ (fb)	Theoretical prediction (fb)
$W^\pm_L W^\pm_L$	$0.24^{+0.40}_{-0.37}$	0.28 ± 0.03
$W^\pm_X W^\pm_T$	$3.25^{+0.50}_{-0.48}$	3.32 ± 0.37
$W^\pm_L W^\pm_X$	$1.40^{+0.60}_{-0.57}$	1.71 ± 0.19
$W^\pm_T W^\pm_T$	$2.03^{+0.51}_{-0.50}$	1.89 ± 0.21

Prospects

- Measurements of all three components simultaneously
  - Currently unreliable as a matter of statistical precision
  - Possible with a larger data set
- Extrapolations of this analysis to a larger integrated luminosity indicates the projections were on the right (conservative) ballpark
- QCD, and more importantly, EWK corrections for each polarization mode are needed in the future
- Polarized VBS in WZ and ZZ channels could be studied in the future
- More precise measurement: talk to the BSM studies (e.g. *arXiv:1907.04722*)

Summary

- **First measurement** of production cross sections of **polarized same-sign EW WW boson pairs**
  - Using full Run-2 dataset

- Report in both WW and parton-parton c.m. frame
  - WW c.m. frame
    - Observed (expected) significance of **2.3 (3.1)** $\boldsymbol{\sigma}$ for $\mathbf{W_L^{\pm}W_X^{\pm}}$ production
    - Observed (expected) limit of **1.17 (0.88) fb** for $\mathbf{W_L^{\pm}W_L^{\pm}}$ production
  - Parton-parton c.m. frame
    - Observed (expected) significance of **2.6 (2.9)** $\boldsymbol{\sigma}$ for $\mathbf{W_L^{\pm}W_X^{\pm}}$ production
    - Observed (expected) limit of **1.06 (0.85) fb** for $\mathbf{W_L^{\pm}W_L^{\pm}}$ production

- Measurements agree with SM predictions
- More to expected with higher luminosity

Thanks!

BACK UP

Data, Triggers and Simulated samples

- Data
  - Full Run-II dataset with 133.5 fb^{-1} of integrated luminosity
    - 16&17: MuonEG, DoubleMuon, DoubleElectron, SingleMuon and SingleElectron / Re-Reco
    - 18: MuonEG, DoubleMuon, SingleMuon and EGamma / Re-Reco for EraABC & PromptReco for EraD

- Triggers
  - Single and Double Lepton triggers
  - ~100% efficiency
  - Single lepton triggers recover 4% efficiency

- Main simulated samples (detailed tables of names and cross section in backup P30-31)
  - 2016
    - QCD SSWW: WpWpJJ_QCD_TuneCUETP8M1_13TeV-madgraph-pythia
    - EWK WZ: WLLJJ_WToLNu_EWK_TuneCUETP8M1_13TeV_madgraph-madspin-pythia8
    - QCD WZ: WZTo3LNu_NJets_TuneCUETP8M1 13TeV-madgraphMLM-pythia8

  - 2017&18
    - QCD SSWW: WpWpJJ QCD TuneCP5 13TeV-madgraph-pythia8
    - EWK WZ: WLLJJ_WToLNu_EWK_TuneCP5_13TeV_madgraph-madspin-pythia8
    - QCD WZ: WZTo3LNu_TuneCP5_13TeV-amcatnloFXFX-pythia8

Simulated Samples (2016)

Process	Dataset Name	Cross Section [pb^{-1}]
$Z/\gamma^* \to l^+l^-(50)$	DYJetsToLL_Pt-50To100_TuneCUETP8M1_13TeV-amcatnloFXFX-pythia8	$354.6*(1921.8*3/5938)$
$Z/\gamma^* \to l^+l^-(50)$	DYJetsToLL_Pt-100To250_TuneCUETP8M1_13TeV-amcatnloFXFX-pythia8	$83.05*(1921.8*3/5938)$
$Z/\gamma^* \to l^+l^-(50)$	DYJetsToLL_Pt-250To400_TuneCUETP8M1_13TeV-amcatnloFXFX-pythia8	$3.043*(1921.8*3/5938)$
$Z/\gamma^* \to l^+l^-(50)$	DYJetsToLL_Pt-400To650_TuneCUETP8M1_13TeV-amcatnloFXFX-pythia8	$0.3921*(1921.8*3/5938)$
$Z/\gamma^* \to l^+l^-(50)$	DYJetsToLL_Pt-650ToInf_TuneCUETP8M1_13TeV-amcatnloFXFX-pythia8	$0.03823*(1921.8*3/5938)$
$Z/\gamma^* \to l^+l^-(50)$	DYJetsToLL_M-50_TuneCUETP8M1_13TeV-madgraphMLM-pythia8	$4958*(1921.8*3/4958)$
$Z/\gamma^* \to 2\tau \to e\mu(50)$	DYJetsToTauTau_ForcedMuEleDecay_M-50_TuneCUETP8M1_13TeV-amcatnloFXFX-pythia8	$1921.8*(0.1741+0.1783)^2$
$Z+\gamma$	ZGTo2LG_TuneCUETP8M1_13TeV-amcatnloFXFX-pythia8	117.864
$ZZ \to 2l2\nu$	ZZTo2L2Nu_13TeV_powheg_pythia8	$0.564*$ *k-factor*
$ZZ \to 4l$	ZZTo4L_13TeV_powheg_pythia8	$1.256*$ *k-factor*
$ZZ \to 2l2q$	ZZTo2L2Q_13TeV_amcatnloFXFX_madspin_pythia8	$3.220*$ *k-factor*
$qq \to WW \to 2l2\nu$	WWTo2L2Nu_13TeV-powheg	$(118.7-3.974)*0.1086*0.1086*9$
$gg \to WW \to 2l2\nu$	GluGluWWTo2L2Nu_MCFM_13TeV	$(3.974*0.1086*0.1086*9*1.4$
$WZ \to 3l\nu$	WZTo3LNu_NJets_TuneCUETP8M1 13TeV-madgraphMLM-pythia8	$4.42965*1.109$
$WZ \to 2l2q$	WZTo2L2Q_13TeV_amcatnloFXFX_madspin_pythia8	$5.595*1.109$
$t\bar{t} \to 2l2\nu 2b$	TTTo2L2Nu_TuneCUETP8M2_ttHtranche3_13TeV-powheg-pythia8	$831.76*0.1086*0.1086*9$
$t\bar{t}Z(qq)$	TTZToQQ_TuneCUETP8M1_13TeV-amcatnlo-pythia8	0.5297
$t\bar{t}Z(ll)$	TTZToLLNuNu_M-10_TuneCUETP8M1_13TeV-amcatnlo-pythia8	0.2529
tW	ST_tW_top_5f_inclusiveDecays_13TeV-powheg-pythia8_TuneCUETP8M1	35.6
$\bar{t}W$	ST_tW_antitop_5f_inclusiveDecays_13TeV-powheg-pythia8_TuneCUETP8M1	35.6
$gg \to ZZ \to 2e2\mu$	GluGluToContinToZZTo2e2mu_13TeV_MCFM701_pythia8	$0.003194*2.3$
$gg \to ZZ \to 2e2\nu$	GluGluToContinToZZTo2e2nu_13TeV_MCFM701_pythia8	$0.001720*2.3$
$gg \to ZZ \to 2e2\tau$	GluGluToContinToZZTo2e2tau_13TeV_MCFM701_pythia8	$0.003194*2.3$
$gg \to ZZ \to 2\mu 2\nu$	GluGluToContinToZZTo2mu2nu_13TeV_MCFM701_pythia8	$0.001720*2.3$
$gg \to ZZ \to 2\mu 2\tau$	GluGluToContinToZZTo2mu2tau_13TeV_MCFM701_pythia8	$0.003194*2.3$
$gg \to ZZ \to 4e$	GluGluToContinToZZTo4e_13TeV_MCFM701_pythia8	$0.001586*2.3$
$gg \to ZZ \to 4\mu$	GluGluToContinToZZTo4mu_13TeV_MCFM701_pythia8	$0.001586*2.3$
$gg \to ZZ \to 4\tau$	GluGluToContinToZZTo4tau_13TeV_MCFM701_pythia8	$0.001586*2.3$
ZZZ	ZZZ_TuneCUETP8M1_13TeV-amcatnlo-pythia8	0.01398
WZZ	WZZ_TuneCUETP8M1_13TeV-amcatnlo-pythia8	0.05565
WWZ	WWZ_TuneCUETP8M1_13TeV-amcatnlo-pythia8	0.16510
$PW^{\pm}PW^{\pm}$ EW	WpWpJJ_EWK_TuneCUETP8M1_13TeV-madgraph-pythia8	0.027
WZ EW	WLLJJ_WToLNu_EWK_TuneCUETP8M1_13TeV_madgraph-madspin-pythia8	0.0176

Simulated Samples (2017 + 2018)

Process	Dataset Name	Cross Section [pb^{-1}]
$Z/\gamma^* \to l^+l^-(50)$	DY1JetsToLL_M-50_LHEZpT_50-150_TuneCP5_13TeV-amcnloFXFX-pythia8	316.6
$Z/\gamma^* \to l^+l^-(50)$	DY1JetsToLL_M-50_LHEZpT_150-250_TuneCP5_13TeV-amcnloFXFX-pythia8	9.543
$Z/\gamma^* \to l^+l^-(50)$	DY1JetsToLL_M-50_LHEZpT_250-400_TuneCP5_13TeV-amcnloFXFX-pythia8	1.098
$Z/\gamma^* \to l^+l^-(50)$	DY1JetsToLL_M-50_LHEZpT_400-inf_TuneCP5_13TeV-amcnloFXFX-pythia8	0.1193
$Z/\gamma^* \to l^+l^-(50)$	DY2JetsToLL_M-50_LHEZpT_50-150_TuneCP5_13TeV-amcnloFXFX-pythia8	169.6
$Z/\gamma^* \to l^+l^-(50)$	DY2JetsToLL_M-50_LHEZpT_150-250_TuneCP5_13TeV-amcnloFXFX-pythia8	15.65
$Z/\gamma^* \to l^+l^-(50)$	DY2JetsToLL_M-50_LHEZpT_250-400_TuneCP5_13TeV-amcnloFXFX-pythia8	2.737
$Z/\gamma^* \to l^+l^-(50)$	DY2JetsToLL_M-50_LHEZpT_400-inf_TuneCP5_13TeV-amcnloFXFX-pythia8	0.4477
$Z/\gamma^* \to l^+l^-(50)$	DYJetsToLL_M-50_TuneCP5_13TeV-amcatnloFXFX-pythia8	6529.0
$Z/\gamma^* \to 2\tau \to e\mu(50)$	DYJetsToTauTau_ForcedMuEleDecay_M-50_TuneCP5_PSweights_13TeV-amcatnloFXFX-pythia8	6505.0
$Z+\gamma$	ZGTo2LG_TuneCUETP8M1_13TeV-amcatnloFXFX-pythia8	117.864
$ZZ \to 2l2\nu$	ZZTo2L2Nu_13TeV_powheg_pythia8	0.5644 * k-*factor*
$ZZ \to 4l$	ZZTo4L_13TeV_powheg_pythia8	1.256 * k-*factor*
$ZZ \to 2l2q$	ZZTo2L2Q_13TeV_amcatnloFXFX_madspin_pythia8	3.688 * k-*factor*
$qq \to WW \to 2l2\nu$	WWTo2L2Nu_NNPDF31_TuneCP5_PSweights_13TeV-powheg-pythia8	12.178
$gg \to WW \to 2l2\nu$	GluGluWWTo2L2Nu_MCFM_13TeV	$(3.974 * 0.1086 * 0.1086 * 9 * 1.4$
$WZ \to 3l\nu$	WZTo3LNu_TuneCP5_13TeV-amcatnloFXFX-pythia8	5.052
$WZ \to 2l2q$	WZTo2L2Q_13TeV_amcatnloFXFX_madspin_pythia8	6.331
$t\bar{t} \to 2l2\nu2b$	TTTo2L2Nu_TuneCP5_PSweights_13TeV-powheg-pythia8	88.29
$t\bar{t}Z(qq)$	TTZToQQ_TuneCP5_13TeV-amcatnlo-pythia8	0.5104
$t\bar{t}Z(ll)$	TTZToLLNuNu_M-10_TuneCP5_13TeV-amcatnlo-pythia8	0.2432
$t\bar{t}W(l\nu)$	TTWJetsToLNu_TuneCP5_13TeV-amcatnloFXFX-madspin-pythia8	0.2149
$t\bar{t}W(qq)$	TTWJetsToQQ_TuneCP5_13TeV-amcatnloFXFX-madspin-pythia8	0.4316
tW	ST_tW_top_5f_inclusiveDecays_TuneCP5_13TeV-powheg-pythia8	34.91
$\bar{t}W$	ST_tW_antitop_5f_inclusiveDecays_TuneCP5_13TeV-powheg-pythia8	34.97
$gg \to ZZ \to 2e2\mu$	GluGluToContinToZZTo2e2mu_13TeV_MCFM701_pythia8	$0.003291 * 2.3$
$gg \to ZZ \to 2e2\nu$	GluGluToContinToZZTo2e2nu_13TeV_MCFM701_pythia8	$0.001772 * 2.3$
$gg \to ZZ \to 2e2\tau$	GluGluToContinToZZTo2e2tau_13TeV_MCFM701_pythia8	$0.00329 * 2.3$
$gg \to ZZ \to 2\mu2\nu$	GluGluToContinToZZTo2mu2nu_13TeV_MCFM701_pythia8	$0.001772 * 2.3$
$gg \to ZZ \to 2\mu2\tau$	GluGluToContinToZZTo2mu2tau_13TeV_MCFM701_pythia8	$0.003289 * 2.3$
$gg \to ZZ \to 4e$	GluGluToContinToZZTo4e_13TeV_MCFM701_pythia8	$0.001405 * 2.3$
$gg \to ZZ \to 4\mu$	GluGluToContinToZZTo4mu_13TeV_MCFM701_pythia8	$0.001402 * 2.3$
$gg \to ZZ \to 4\tau$	GluGluToContinToZZTo4tau_13TeV_MCFM701_pythia8	$0.001407 * 2.3$
ZZZ	ZZZ_TuneCP5_13TeV-amcatnlo-pythia8	0.01398
WZZ	WZZ_TuneCP5_13TeV-amcatnlo-pythia8	0.05565
WWZ	WWZ_TuneCP5_13TeV-amcatnlo-pythia8	0.16510
$PW^{\pm}PW^{\pm}$ EW	WpWpJJ_EWK_TuneCP5_13TeV-madgraph-pythia8	0.027
WZ EW	WLLJJ_WToLNu_EWK_TuneCP5_13TeV_madgraph-madspin-pythia8	0.0176

Polarized $W^{\pm}W^{\pm}$ scattering: Object Selections

Follow the same selections in SMP-19-012 *phys.lett.b.2020.135710*

- Muons
  - two selected leptons: $|\eta| < 2.4$, $p_T > 20$ GeV
    - 2016: **cut-based** tight ID & PF relative isolation < 0.15
    - 2017: muon **MVA** tight WP & mini isolation tight WP
    - 2018: **cut-based** tight ID & mini isolation tight WP
  - Fakeable object: tight ID, PF relative isolation < 0.40 & tracker relation isolation < 0.40, $|\eta| < 2.4$, $p_T > 10$ GeV
  - Veto object: **cut-based loose** ID, $|\eta| < 2.4$, $p_T > 10$ GeV
- Electrons
  - two selected leptons: $|\eta| < 2.5$, $p_T > 20$ GeV
    - 2016,17,18: electron **MVA** tight WP & triple charge requirement
  - Fakeable object: HLT-safe WP, $|\eta| < 2.5$, $p_T > 10$ GeV
  - Veto object: **cut-based loose** ID, $|\eta| < 2.5$, $p_T > 10$ GeV
- Tau: Veto hadronically decay tau
- E_T^{miss}
  - Particle-Flow E_T^{miss} using PF candidates
  - type-I correction applied
- Jets
  - anti-kT with R = 0.4 PF jets, $|\eta_j| < 4.5$
- Anti B-tagging
  - 2016,17,18: **DeepCSV**, medium WP

Data Measurements

- Trigger efficiencies
  - Measured using E_T^{miss} related trigger paths as a combination of trigger paths
  - Tiny effect for high pT analyses
- Nonprompt rates
  - Measured using QCD enriched samples
  - Critical to keep backup triggers alive
- Lepton efficiency scale factors
  - measured using $Z \rightarrow ll$ events
- Electron wrong charge efficiency
  - Measured using $Z \rightarrow ee$ events as a function of η
- Known data issues
  - Applied pre-firing map probabilities: ~5/15% effect in 2016/2017
  - Applied 2017 E_T^{miss} recipe to improve its behavior, tiny impact for analyses with real E_T^{miss}

Nonprompt Leptons

- Fake rate ε_{fake}
  - Defined as the efficiency for fakeable objects to pass full lepton selection
  - Measured in a QCD-enriched sample
  - η and p_T dependence (2D e/μ fake rate for each year in backup slide 35)

- Extrapolate the background yields
  - from "tight+loose" and "loose+loose" data events in "SR"
  - by weighted

"tight+loose": $$w_i = \frac{\epsilon_{\text{fake}}(p_{\text{Ti}}, \eta_i)}{1 - \epsilon_{\text{fake}}(p_{\text{Ti}}, \eta_i)}$$

"loose+loose": $$(w_{ij} = \frac{\epsilon_{\text{fake}}(p_{\text{Ti}}, \eta_i)}{1 - \epsilon_{\text{fake}}(p_{\text{Ti}}, \eta_i)} \times \frac{\epsilon_{\text{fake}}(p_{\text{Tj}}, \eta_j)}{1 - \epsilon_{\text{fake}}(p_{\text{Tj}}, \eta_j)})$$

  - and with real lepton from simulation subtraction

$$N^{non-prompt} = \sum_i w_i^{data} - \sum_i w_i^{MC} - \sum_{i,j} w_{ij}^{data} + \sum_{i,j} w_{ij}^{MC}$$

Nonprompt Rate

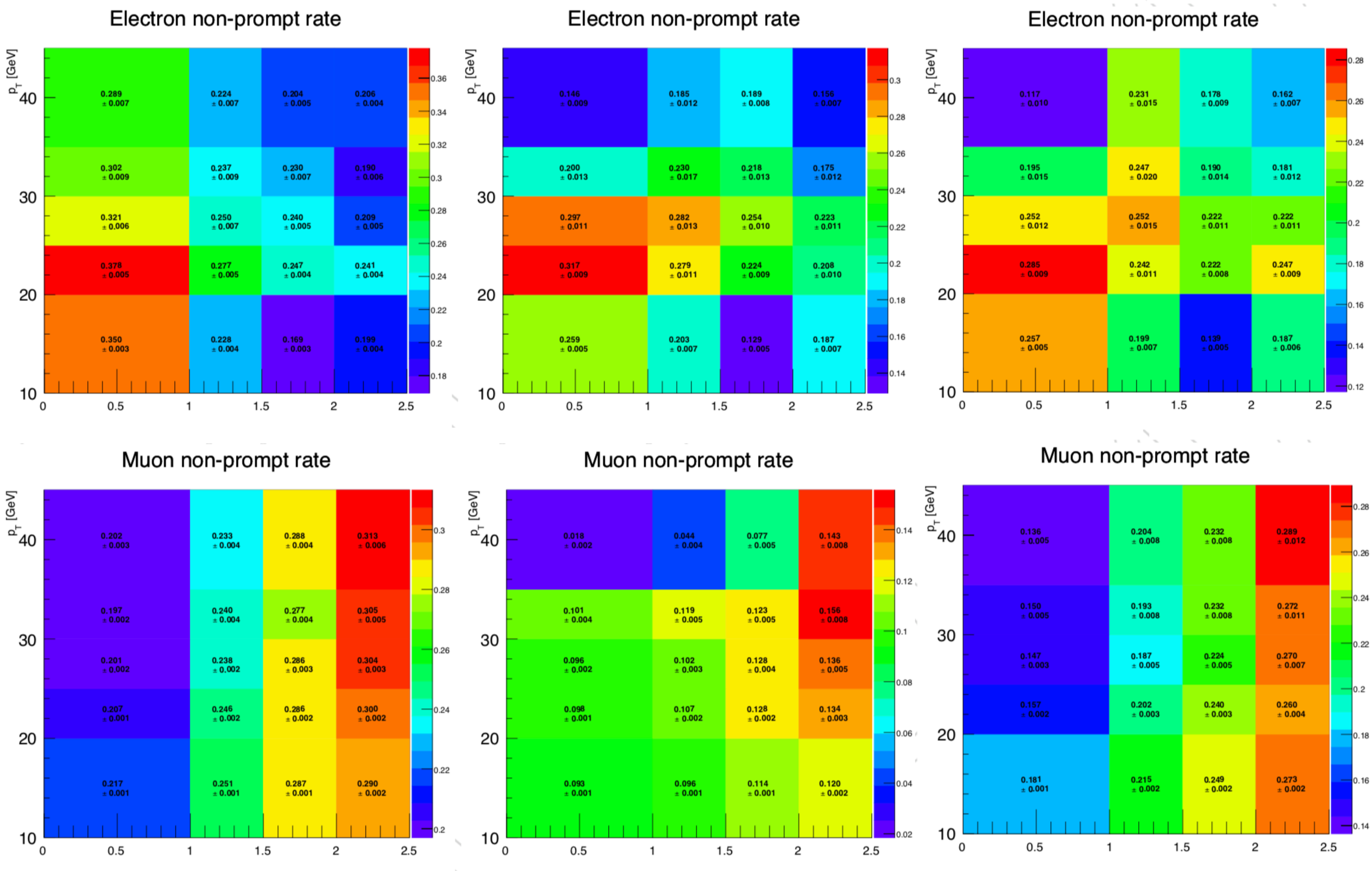

Wrong Sign Lepton Pairs

- Charge mis-ID rate ε_{sim} and ε_{data}
  - Studies by the muon POG show that the charge mis-ID rate for **muons** is **negligible**
  - For **electrons**
    - Measured from *Z* plus jets sample with two electrons
    - As ratio between same sign and opposite sign dielectron events
    - similarly in data
- Estimate the background yields by applying charge mis-ID scale factor: $\varepsilon_{data}/\varepsilon_{sim}$ to two opposite-sign simulated events in "SR"

$\|\eta\|$-range	Data	MC	Scale factor
		2016	
0.0-0.5	0.0023 ± 0.0004	0.0016 ± 0.0003	1.45 ± 0.27
0.5-1.0	0.0077 ± 0.0006	0.0068 ± 0.0005	1.14 ± 0.11
1.0-1.5	0.0345 ± 0.0013	0.0368 ± 0.0012	0.94 ± 0.05
1.5-2.0	0.2251 ± 0.0037	0.2296 ± 0.0033	0.98 ± 0.02
2.0-2.5	0.2174 ± 0.0044	0.2224 ± 0.0040	0.98 ± 0.03
		2017	
0.0-0.5	0.0025 ± 0.0004	0.0013 ± 0.0003	1.96 ± 0.28
0.5-1.0	0.0053 ± 0.0005	0.0052 ± 0.0004	1.01 ± 0.12
1.0-1.5	0.0302 ± 0.0011	0.0194 ± 0.0009	1.56 ± 0.06
1.5-2.0	0.1067 ± 0.0023	0.0701 ± 0.0017	1.52 ± 0.03
2.0-2.5	0.1596 ± 0.0036	0.1093 ± 0.0026	1.46 ± 0.03
		2018	
0.0-0.5	0.0019 ± 0.0003	0.0012 ± 0.0002	1.67 ± 0.25
0.5-1.0	0.0059 ± 0.0004	0.0027 ± 0.0003	2.19 ± 0.13
1.0-1.5	0.0246 ± 0.0009	0.0177 ± 0.0007	1.39 ± 0.05
1.5-2.0	0.1219 ± 0.0020	0.0877 ± 0.0016	1.39 ± 0.02
2.0-2.5	0.1603 ± 0.0027	0.1257 ± 0.0022	1.28 ± 0.02

Polarized $W^{\pm}W^{\pm}$ scattering: Signal BDTs

- Signal BDTs to separate different polarization configurations
  - Same input variables for two settings (i) LL against (LT+TT) and (ii) (LL+LT) against TT

	Variables	Definitions
jj variables (3)	$\Delta\Phi_{jj}$	Difference in Φ between the leading and trailing jets
	p_T^{j1}	P_T of the leading jet
	p_T^{j2}	P_T of the trailing jet
V(l) variables(6)	p_T^{l1}	P_T of the leading lepton
	p_T^{l2}	P_T of the trailing lepton
	$\Delta\Phi_{ll}$	Difference in Φ between the two leptons
	m_{ll}	Dilepton mass
	p_T^{ll}	Dilepton P_T
	m_T^{WW}	Transverse WW diboson mass
V-j mix variables(6)	$z^*_{\ell_1}$	Zeppenfeld variable of the leading lepton
	$z^*_{\ell_2}$	Zeppenfeld variable of the trailing lepton
	p_T^{miss}	Missing transverse momentum
	$\Delta R_{j1,ll}$	ΔR between the leading jet and the dilepton system
	$\Delta R_{j2,ll}$	ΔR between the trailinging jet and the dilepton system
	$(p_T^{l1} p_T^{l2})/(p_T^{j1} p_T^{j2})$	Ratio of P_T products between leptons and jets

Polarized W±W± scattering: Inclusive BDTs

- Inclusive BDT to isolate EW W±W± signal from nonVBS backgrounds
  - 10 Input variables for training

	Variables	Definitions
jj variables (5)	m_{jj}	The mass of the leading and trailing jets
	$\|\Delta\eta_{jj}\|$	Absolute difference in rapidity of the leading and trailing jets
	$\Delta\Phi_{jj}$	Difference in Φ of the leading and trailing jets
	p_T^{j1}	P_T of the leading jet
	p_T^{j2}	P_T of the trailing jet
V(l) variables(2)	p_T^{l1}	Leading lepton pT
	p_T^{ll}	Dilepton pT
V-j mix variables(3)	$z^*_{\ell_1}$	Zeppenfeld variable of the leading lepton
	$z^*_{\ell_2}$	Zeppenfeld variable of the trailing lepton
	p_T^{miss}	Missing transverse momentum

Polarized $W^{\pm}W^{\pm}$ scattering: Signal Extraction

- Simultaneously fit on several distributions across all signal and control regions

- **SSWW (Signal) Region**: 2D distribution
  - **Signal BDT** : 5 bins
    - Fitting for LL v.s. XT and LX v.s. TT separately
  - **Inclusive BDT** : 5 bins

- **Nonprompt (Control) Region**: 4 bins
  - **mjj** : [500, 800, 1200, 1800, ∞] GeV

- **WZ (Control) Region**: 8 bins
  - **mjj** : [500, 800, 1200, 1800, ∞] GeV

- **WZb(tZq) (Control) Region**: 4 bins
  - **mjj** : [500, 800, 1200, 1800, ∞] GeV

- **ZZ (Control) Region**: 4 bins
  - **mjj** : [500, 800, 1200, 1800, ∞] GeV

mjj is the variable most sensitive to EW $W^{\pm}W^{\pm}$ process are used